Available online at www.sciencedirect.com
ScienceDirect
Journal of Power Sources 171 (2007) 464–470
JOURNAL OF POWER SOURCES
www.elsevier.com/locate/jpowsour

Cycle analysis of low and high H_2 utilization SOFC/gas turbine combined cycle for CO_2 recovery

Takuto Araki [a,*], Takuya Taniuchi [a], Daisuke Sunakawa [a], Mitsuyuki Nagahama [a], Kazuo Onda [a], Toru Kato [b]

[a] *Department of Electrical and Electronic Engineering, Toyohashi University of Technology, 1-1 Hibarigaoka, Tenpaku-cho, Toyohashi-shi, Aichi-ken 441-8580, Japan*
[b] *National Institute of Advanced Industrial Science and Technology (AIST), Japan*

Received 6 November 2006; received in revised form 25 May 2007; accepted 4 June 2007
Available online 13 June 2007

Abstract

A major factor in global warming is CO_2 emission from thermal power plants, which burn fossil fuels. One technology proposed to prevent global warming is CO_2 recovery from combustion flue gas and the sequestration of CO_2 underground or near the ocean bed. Solid oxide fuel cell (SOFC) can produce highly concentrated CO_2, because the reformed fuel gas reacts with oxygen electrochemically without being mixed with air in the SOFC. We therefore propose to operate multi-staged SOFCs with high utilization of reformed fuel to obtain highly concentrated CO_2. In this study, we estimated the performance of multi-staged SOFCs considering H_2 diffusion and the combined cycle efficiency of a multi-staged SOFC/gas turbine/CO_2 recovery power plant. The power generation efficiency of our CO_2 recovery combined cycle is 68.5%, whereas the efficiency of a conventional SOFC/GT cycle with the CO_2 recovery amine process is 57.8%.

Keywords: Multi-staged SOFC; CO_2 recovery; Gas turbine combined power generation; High fuel utilization; Amine process

1. Introduction

Emission of CO_2 into the atmosphere is a major cause of global warming in recent years, and technology is currently being investigated for the recovery of CO_2 released from thermal power plants. Meanwhile, research and development of fuel cells is advancing rapidly, since they have greater efficiency and cause less atmospheric pollution than conventional power generation methods. SOFC have a high operating temperature of about 1000 °C, so the recovery of high temperature exhaust heat with a gas turbine (GT) is being investigated in order to construct a high efficiency combined cycle. In most cases, however, the fuel released from an SOFC is burned with air, so CO_2 is included in the exhaust gas from the system. Therefore, investigations have been made of the recovery and liquefaction of CO_2 even in SOFC power generation, and the sequestration of this CO_2 underground or underwater [1].

Since oxygen moves to the anode in an SOFC, the fuel exhaust gas becomes CO_2 and H_2O only if a complete reaction occurs at the anode. When H_2O is condensed and removed, high concentration CO_2 can be obtained and there is no need to use the amine process to absorb and isolate CO_2 from the combustion flue gas in which N_2 is mixed. However, when an SOFC is running with a high fuel utilization ratio, the cell voltage drops and the power generation efficiency declines. Therefore, we set a separate SOFC that operates with high fuel utilization downstream of an SOFC that operates with the conventional fuel utilization. In cases when the electromotive force of the high fuel utilization SOFC is small and current density is low, it might be necessary to supply electric power to operate the SOFC as an oxygen pump and forcefully transfer oxygen to the fuel side. Since the details were not reported by Lokurlu et al. [1], we herein report the following investigations.

In fuel cells, fuel is separated from air and made to react with oxygen. Therefore, if the reaction is nearly complete, high concentration CO_2 can be obtained without an isolation process. We investigated an SOFC/GT combined generation cycle for CO_2 recovery, in which an additional SOFC that operates with

* Corresponding author. Tel.: +81 532 44 6728; fax: +81 532 44 6728.
E-mail address: araki@eee.tut.ac.jp (T. Araki).

0378-7753/$ – see front matter © 2007 Elsevier B.V. All rights reserved.
doi:10.1016/j.jpowsour.2007.06.002

high fuel utilization is placed after a conventional fuel utilizing SOFC. In this cycle, the CO_2 concentration in the depleted fuel after H_2O is removed was set above 99.95%. At this time, if the additional SOFC operates in a single stage, the Nernst electromotive force at the downstream becomes too small, as described below, and the electric current is concentrated upstream, so that almost no current flows downstream. Therefore, the additional SOFC is divided into multiple stages and operated so that the fuel utilization rises sequentially. In addition, to serve as reference to the proposed cycle, we also considered a conventional SOFC/GT cycle [2], which burns depleted fuel and recovers CO_2 by the amine process. The analytical method for the SOFC reported here is partially improved from that in a previous report, and gas diffusion in the flow direction and the direction perpendicular to the cell is considered.

2. Constitution and analysis method of SOFC and its combined cycle

2.1. Constitution and calculation method of high and low fuel utilization SOFCs

This analysis considered the same planar type SOFCs previously reported [2] for both the high and low fuel utilization SOFCs. The material of electrolyte is YSZ, and electrode of anode and cathode are Ni-YSZ cermet and $LaSrMnO_3$, respectively. Activation overpotential $V_{act,air}$ (V) and $V_{act,fuel}$ (V) for the air and fuel electrodes are given by the following equations for current density i_e (A cm^{-2}) through electrolyte [3].

$$i_e = \frac{RT}{3F} s_{fuel} \left\{ \exp\left(\frac{2FV_{act,fuel}}{RT_e}\right) - \exp\left(\frac{-FV_{act,fuel}}{RT_e}\right) \right\} \quad (1)$$

$$i_e = \frac{RT}{4F} s_{air} \left\{ \exp\left(\frac{2FV_{act,air}}{RT_e}\right) - \exp\left(\frac{-2FV_{act,air}}{RT_e}\right) \right\} \quad (2)$$

Here, T_e is electrode temperature, R the gas constant, F the Faraday constant, s_{air} and s_{fuel} are the electrode interface conductivity of the cathode and anode electrodes, respectively, which are given as follows [4,5]

$$s_{fuel} = 125.6 \times 10^{10} \exp\left(\frac{-138000}{RT}\right) P_{O_2,fuel}^{0.15} \quad (3a)$$

$$s_{air} = 62.7 \times 10^{6} \exp\left(\frac{-136000}{RT}\right) P_{O_2,air}^{0.5} \quad (3b)$$

When an operating SOFC is in a high fuel utilization mode, in which the reduction state is decreased, doubt remains as to whether the same equation for activation overpotential can be used. However, since no overpotential equation has been published for high fuel utilization, and V–i characteristics change almost linearly from power generation mode to high-temperature steam electrolysis mode [6,7], it was assumed that the previous activation overpotential would give a good approximation even in the high fuel utilization condition. In addition, the exhaust gas at the anode exit of SOFC was assumed to react

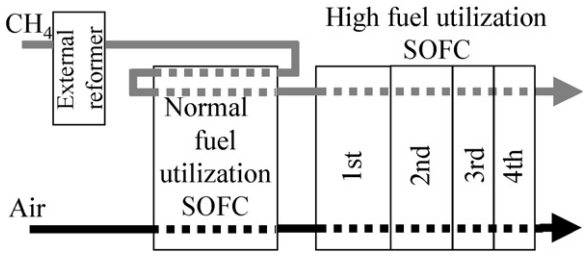

Fig. 1. Structural diagram of normal and high fuel utilization SOFC.

electrochemically until a very high fuel utilization ratio, which is equivalent to the CO_2 concentration of 99.95% [8] obtained by the amine process, when the water vapor of the depleted fuel is eliminated.

In the normal fuel utilization SOFC, 50% of fuel was set to be reformed at an external reformer and the remaining 50% was internally reformed to cool the SOFC, similarly to our previous study. Further, since the shift reaction is considered to be fast enough, equilibrium in the shift reaction was assumed in the external reformer and internal fuel reforming flow channel. Based on these operating conditions, a high fuel utilization SOFC for CO_2 recovery was positioned downstream of a normal fuel utilization SOFC, as shown in Fig. 1. The fuel and air released from the normal SOFC enter the high fuel utilization SOFC from the first to fourth stage, and since current density declines together with the decrease in Nernst electromotive force, the average current density is made to drop sequentially for the reaction of low concentration fuel. Fuel and air are assumed to flow without any heat loss between stages of the high fuel utilization SOFC.

The diffusion coefficient of H_2 is larger than that of other gases, so present analytical model was modified to allow consideration of the diffusion of H_2 in the cell flow direction. Further, the concentration overpotential was neglected in our previous study because it was small, but since the diffusion flux decreases together with decreasing H_2 concentration, the concentration overpotential was also considered in this study. The concentration distribution within porous diffusion electrodes was taken to be a one-dimensional flow and analyzed with a non-isobaric gas diffusion model [9] to obtain the concentration overpotential. When hydrogen and water vapor flow within the diffusion electrode are countercurrents, the distributions of pressure and concentration can be described as below. When the molar flux in the perpendicular direction to membrane y of component 1 (hydrogen) and component 2 (water vapor) at the anode are taken to be N_1 and N_2, respectively, the change of total pressure p in direction y is obtained from the following equation, where μ is the viscosity, ε the porosity, τ the tortuosity and m_i is the molecular weight of gas species i.

$$\frac{dp}{dy} = \frac{-(N_t - \beta N_1)RT}{D_{22}} \quad (4)$$

Here, $N_t = N_1 + N_2$, $\beta = 1 - D_1/D_2$

$$D_{22} = D_2 \left\{ 1 + \left(\frac{X_1}{D_1} + \frac{X_2}{D_2} \right) \frac{Bp}{\mu} \right\},$$

$$D_i = \left(\frac{\varepsilon}{\tau} \right) \left(\frac{d}{3} \right) \left\{ \frac{8RT}{(\pi m_i)} \right\}^{0.5},$$

$$B = \left(\frac{\varepsilon}{\tau} \right) \left(\frac{d^2}{32} \right), \quad X_2 = 1 - X_1$$

The change in mole fraction X_1 in the y direction is obtained by the following equation.

$$\frac{dX_1}{dy} \frac{\alpha p D}{RT} = -N_1 + X_1 \alpha N_t + (N_t - \beta N_1) \times \left\{ \alpha D X_1 + \frac{X_1(1-\alpha)Bp}{\mu} \right\} \frac{1}{D_{22}} \quad (5)$$

Here, $\alpha = D_1/(D_1 + D)$ and D are the two-component diffusion coefficients of components 1 and 2 within the electrode.

On the other hand, the concentration overpotential at the cathode is obtained if solved with oxygen as component 1, nitrogen as component 2, and $N_2 = 0$. The concentration overpotential is obtained by iterative computation so that each type of active material in the flow channel, which was divided into the control volume, moves through the diffusion electrode in amounts appropriate to the current density distribution.

2.2. System configuration

Fig. 2 shows the system configuration of the SOFC/GT combined cycle for CO_2 recovery investigated in this study. The configuration of cell except for the length is same as previous report [2], in particular, channel width is 2.0 mm and cathode channel height is 1.0 mm. A high fuel utilization SOFC is placed after a normal fuel utilization SOFC, methane is 50% reformed in the external reformer and supplied to the normal fuel utilization SOFC, and nearly 100% reformed in the internal reforming flow channel. The outlet gases from the normal utilization SOFC are each partially recirculated, and the remaining gases are led to the high utilization SOFC. Recirculated fuel self-supplies water vapor for reformation, and recirculated air evens the SOFC temperature distribution [2]. The high temperature blower for recirculation is as subject for development as some national projects are developing it for MCFC and SOFC. The fuel released from the high utilization SOFC regeneratively exchanges heat through the external reformer and preheaters 1 and 2. Then, H_2O is condensed and separated at the pressure of 1 MPa without any decompression and further compressed to get liquid CO_2. Meanwhile, the air released from the high utilization SOFC undergoes regenerative heat exchange through preheater 1, expands to atmospheric pressure generating power at GT, exchanges heat regeneratively through preheater 2, and is released into the atmosphere. GT drives an air compressor and methane compressor and generator to produce electrical power by the remaining energy.

2.3. Methods for cycle analysis and calculation conditions

The operating conditions of the balance of plant (BOP) other than the SOFCs are calculated based on the enthalpy balance at the inlets and outlets of each BOP, as shown in Eq. (6).

$$\sum_i M_i \left\{ \int_{T_0}^{T_{in}} Cp_i dT + \Delta H_i(T_0) \right\} \pm Q = \sum_j M_j \left\{ \int_{T_0}^{T_{out}} Cp_j dT + \Delta H_j(T_0) \right\} \quad (6)$$

Here, M_i is gas molar flow rate of gas species i, Cp the specific heat at constant pressure, $\Delta H(T_0)$ the enthalpy of formation at reference temperature T_0, T_{in} and T_{out} are the temperatures at component inlet and outlet, respectively, and Q is input or output energy. GT output and compressor and blower input are estimated from the following equations.

$$W_{Gas\_Turbine} = \sum_i M_i Cp_i T_{in} (1 - \phi^{-(\kappa-1)/\kappa}) \eta_{GT} \quad (7)$$

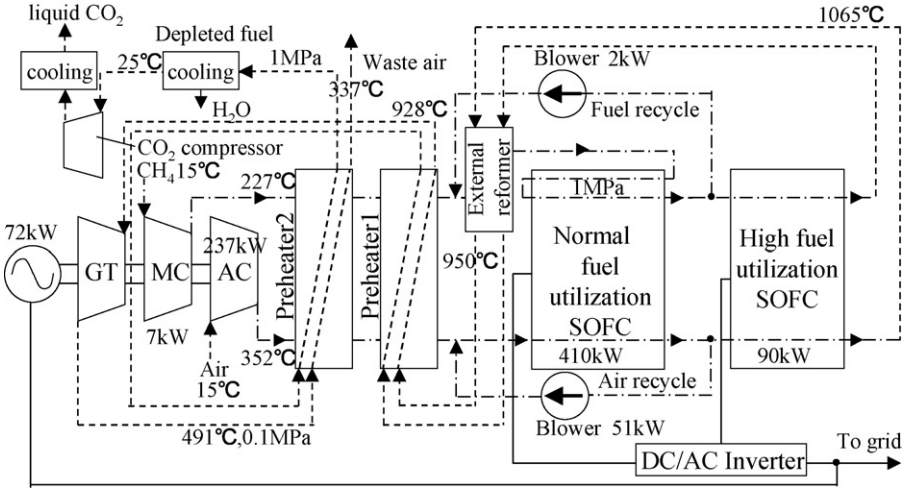

Fig. 2. SOFC/GT combined cycle for CO_2 recovery.

Table 1
Various efficiencies, heat losses and operating conditions of SOFC system

Component	Efficiency, heat loss, operating condition
Normal fuel utilization SOFC	
Fuel utilization ratio [%]	90
Air utilization ratio [%]	30
Average cell temperature [°C]	900
Average current density [A cm^{-2}]	0.3
Fuel recirculation ratio [%]	50
Air recirculation ratio [%]	80
Cell pressure [MPa]	1
Heat loss at SOFC [%]	1
η_{GT} [%]	87
η_{Comp}, η_{Blow} [%]	77
Compression ratio of blower	1.05
Conversion efficiency of inverter [%]	95
Heat loss at preheater 1, 2 and external reformer [%]	3

$$W_{\text{Compressor,Blower}} = \sum_i M_i Cp_i T_{in} \frac{(\phi^{(\kappa-1)/\kappa} - 1)}{\eta_{\text{Comp,Blow}}} \quad (8)$$

Here, ϕ is pressure ratio, κ the specific heat ratio, η_{GT} the adiabatic efficiency of gas turbine, and $\eta_{\text{Comp, Blow}}$ is adiabatic efficiency of compressor and blower. The specific heat and specific heat ratio used here are the means of the respective inlets and outlets.

In the normal fuel utilization SOFC, the air recirculation ratio is set somewhat high at 80% to make the temperature distribution uniform, the fuel utilization ratio is set somewhat high at 90% even in the former stage with the aim of CO_2 recovery, and the other operating conditions are determined the same as in our previous study. In the high fuel utilization SOFC, fuel utilization ratio is set at 80–90% with an appropriate cell length of 4–12 cm. Average current density is decreased sequentially from 0.1 to 0.003 A cm^{-2} together with the decreasing Nernst electromotive force.

SOFC performance is calculated in a single cell assuming an adiabatic boundary condition, but a heat loss of 1% in heat input base was presumed before the normal fuel utilization SOFC stack. Further, 10% of exchange heat was supplied at preheater 1, and the remaining 90% was supplied at preheater 2 to preheat the fuel and air up to SOFC inlet temperature. The above conditions are summarized together with other conditions in Table 1.

3. Numerical results and discussions

3.1. Power generation characteristics of normal and high fuel utilization SOFCs

Fig. 3 shows the potential, current density, and electrolyte temperature distributions in a normal fuel utilization SOFC. The electrolyte temperature (as a representative cell temperature) becomes higher downstream by the overpotential heating, so the resistive activation overpotentials become smaller in the

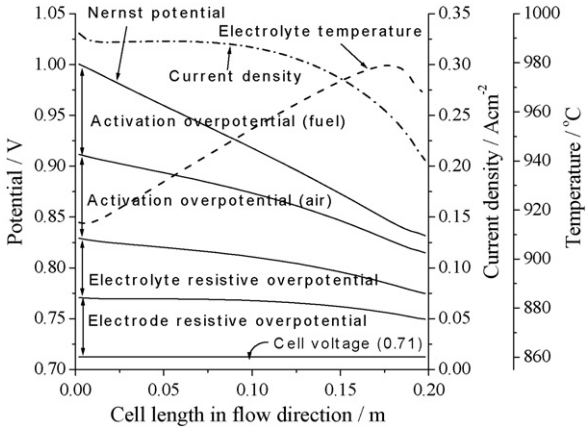

Fig. 3. Potential, current density and temperature distributions in the flow direction at normal fuel utilization SOFC.

downstream region. The temperature decreases near the outlet, because internal reformation absorbs heat. As the fuel is consumed progressively along the flow direction, the hydrogen partial pressure drops, so current density also decreases due to decreasing Nernst electromotive force.

If only one stage of the high fuel utilization SOFC is used for further reaction of the remaining 10% of fuel for CO_2 recovery, the Nernst electromotive force decreases rapidly along the flow, and the current is concentrated upstream with almost no current downstream. Therefore, the high utilization SOFC was divided into four parts matched to the decrease in Nernst electromotive force, and the cell voltage was decreased sequentially in an attempt to make current density as smooth as possible. These distributions of potential, current density, and electrolyte temperature for the first through fourth stages are shown in Figs. 4–7, respectively. Even though the average current density i_{ave} decreases from 0.11 to 0.0036 A cm^{-2}, the current density along the flow direction decreases greatly towards outlet, and the cell voltage also decreases sequentially from 0.60 to 0.28 V from the first to the fourth stage. The anode overpotential is relatively small, because the reducing atmosphere becomes weak together with increasing oxygen concentration, and consequently the surface conductivity increases [2]. The overpotential at the anode

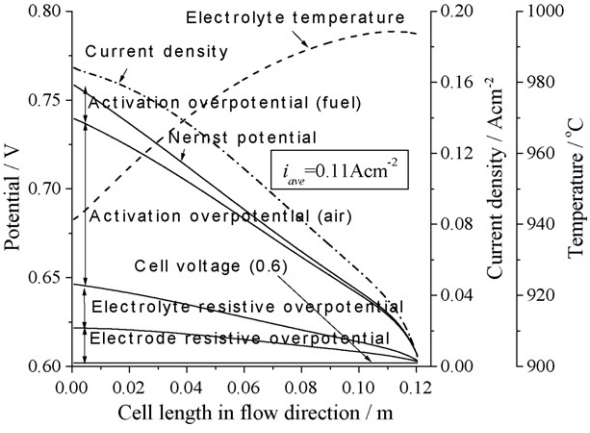

Fig. 4. Potential, current density and temperature distributions in the flow direction at high fuel utilization SOFC (first stage).

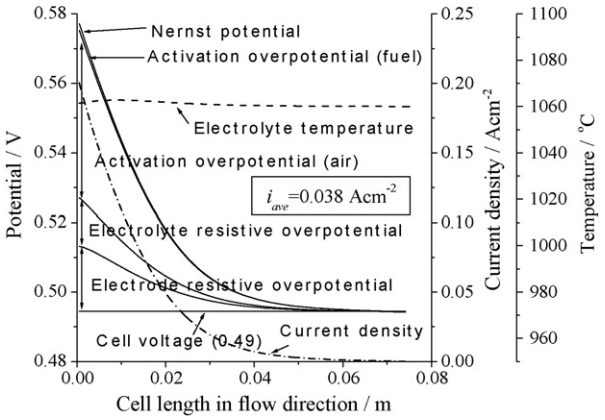

Fig. 5. Potential, current density and temperature distributions in the flow direction at high fuel utilization SOFC (second stage).

with weakening of the reducing atmosphere may need further investigation, including studies on high-temperature water vapor electrolysis [5,6]. Differently from the normal utilization SOFC, temperature rises monotonically in the flow direction because there is no internal reformation, but the temperature rise is saturated due to the decreasing overpotential heat. As described

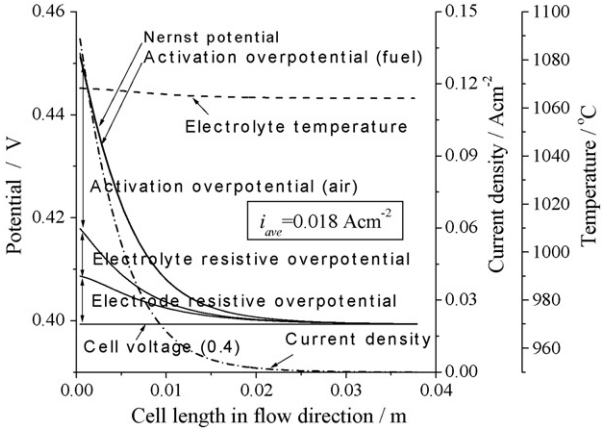

Fig. 6. Potential, current density and temperature distributions in the flow direction at high fuel utilization SOFC (third stage).

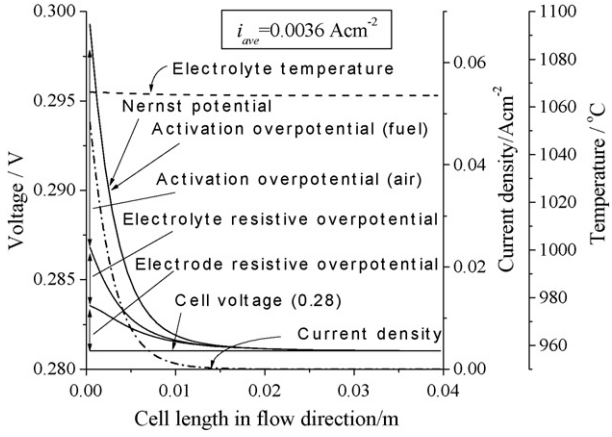

Fig. 7. Potential, current density and temperature distributions in the flow direction at high fuel utilization SOFC (fourth stage).

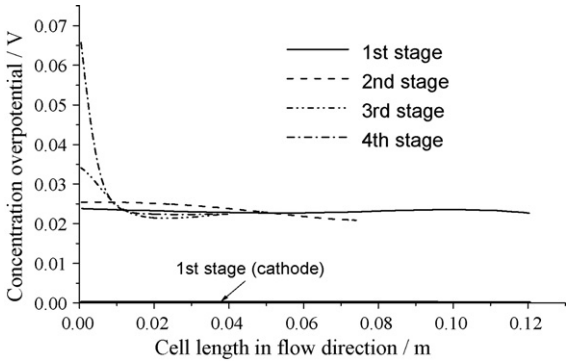

Fig. 8. Concentration overpotential distribution in the flow direction at high fuel utilization SOFC.

above, the total fuel utilization after the fourth stage is 99.98%, and when H_2O is condensed and eliminated, the CO_2 concentration becomes 99.95%.

3.2. Effect of hydrogen diffusion

The concentration overpotentials, which represent the concentration distribution in the diffusion electrode calculated for a high utilization SOFC, are shown in Fig. 8. In the first and second stages of high utilization SOFC, the concentration overpotential is about 25 mV, almost constant along the flow direction. The anode concentration overpotential is relatively large and the cathode concentration overpotential is small. For simplicity of the cycle analysis, concentration overpotential in the normal utilization SOFC was not considered. In the third and fourth stages of the high utilization SOFC, current is focused upstream and concentration overpotential becomes large there. The maximum concentration overpotential was 65 mV at the fourth stage inlet.

Meanwhile, current density distribution and concentration overpotential in the fourth stage of the high utilization SOFC are shown in Fig. 9, considering the effect of hydrogen diffusion in the cell flow direction, which was neglected in our previous study. The effect of concentration overpotential is also shown in Fig. 9. The hydrogen diffusion along the cell flow direction, which is proportional to the gradient of hydrogen concentration,

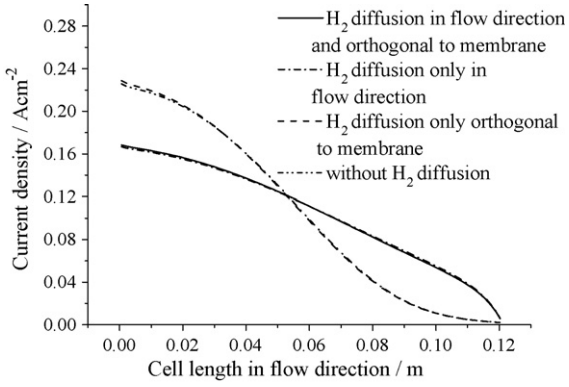

Fig. 9. Effect of H_2 diffusion on current density distribution at the first stage of the high fuel utilization SOFC.

Table 2
Various generation efficiencies and auxiliary power rate

Total	Power generation/auxiliary power [%]	
	(1) High/low fuel utilization SOFCs/GT 68.5(%)	(2) Conventional SOFC/GT 57.8(%)
Normal utilization SOFC	+55.6(%)	+55.6(%)
Fuel compressor	−9.8	−9.8
Air compressor	−32.3	−32.3
Methane recirculation blower	−0.3	−0.3
Air recirculation blower	−7.0	−7.0
High utilization SOFC	+12.3	–
Gas turbine (net)	+52.0% (+2.6%)	+54.6% (+5.2%)
CO_2 compressor	−2.0	−2.8
CO_2 recovery by amine process		
Required heat duty (heat efficiency)	–	−74.6
Required electric power	–	−0.3

affects current density more strongly as the hydrogen concentration becomes thinner and the current density change becomes larger. The effect of hydrogen diffusion is biggest in the fourth stage of the high utilization SOFC and decreases in order in the third and second stages, however, it is better not to neglect the effect in all of the high utilization SOFC. On the other hand, there is almost no effect on the current distribution caused by hydrogen diffusion in the normal utilization SOFC, because the concentration gradient is small. Fig. 9 shows that concentration overpotential has little effect on the current distribution.

3.3. SOFC/GT combined cycle for CO_2 recovery

Fig. 2 also shows calculated temperatures and power losses of a 500 kW class SOFC/GT combined cycle with high fuel utilization SOFC to make CO_2 recovery easier. Calculated results related to power generation efficiencies and other related operating conditions are arranged under (1) in Table 2. For reference, Fig. 10 shows the calculated results of a conventional SOFC/GT cycle using the amine process to recover CO_2 from exhaust gas, where the depleted fuel from SOFC is burned with the depleted air for regenerative heating, reforming and GT power generation. Calculated results related to generation efficiencies and operating conditions are shown in column (2) in Table 2. Here, we referred to Steinberg et al. [10] for the necessary amount of heat and ancillary power for the amine process. The amount of heat necessary for the amine process was sufficiently provided by the flue gas from the SOFC/GT cycle.

A comparison of cycle (1) and (2) shows that output from GT under (1) was small because the high pressure gas released from the SOFC could not drive the GT. Compared with the CO_2 compression power under (2), which compresses from atmospheric pressure, the compression power under (1) was relatively small since the compression can start from the SOFC pressure of 1.0 MPa to the CO_2 liquefying pressure of 7.3 MPa. Further, 0.3% of the electricity was consumed as the auxiliary power in the amine process under (2), but GT power output was about twice as high as in cycle (1). However, since electrical output of 12.3% was produced from the high fuel utilization SOFC in cycle (1), the overall generation efficiency of cycle (1) was

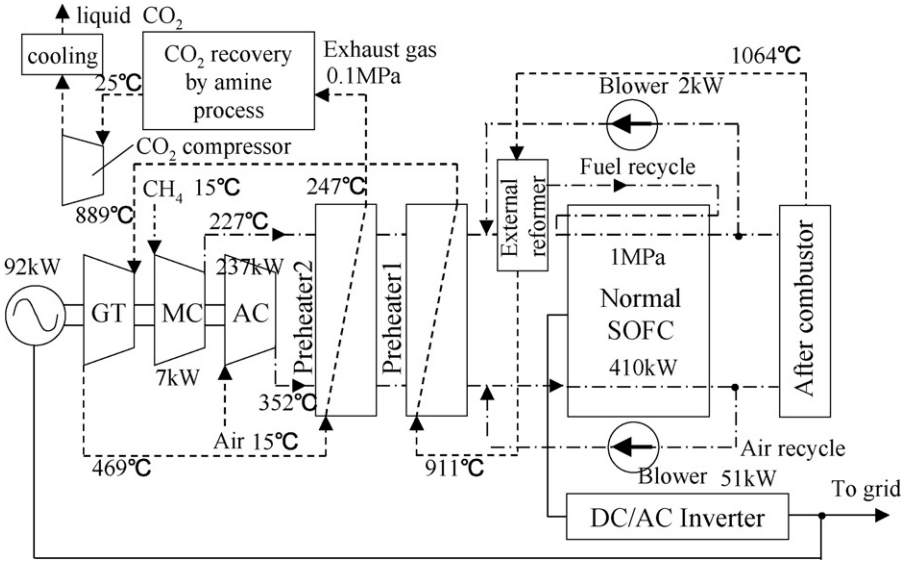

Fig. 10. SOFC/GT combined cycle for CO_2 recovery by amine process.

found to be about 10% higher than that of cycle (2). Since the performance of SOFC under high fuel utilization has not been studied for CO_2 recovery, the high fuel utilization SOFC needs to be experimentally verified as an option for CO_2 recovery. The anode overpotential by Eqs. (2) and (3) is verified by experiment where oxygen partial pressure P_{O_2} is up to 10^{-9} Pa, but the P_{O_2} for our case in Fig. 7 (fourth stage) is 1.5 Pa. The durability of the cell, especially Ni-YSZ in such reduction state, should be also examined.

4. Conclusion

We proposed placement of a high fuel utilization SOFC, where the CO_2 concentration of depleted fuel is more than 99.95% after removing H_2O, downstream of a conventional SOFC to recover CO_2 with high power generation efficiency. In this cycle, no additional equipment such as amine process is necessary for CO_2 recovery and separation. The high fuel utilization SOFC was divided into four stages to avoid concentration of current. Also, the hydrogen diffusion along the flow direction and perpendicular to the electrolyte film were considered in the cycle analysis of a 500 kW class SOFC/GT combined cycle, and the hydrogen diffusion at the third and fourth stage SOFC, where current was apt to concentrate upstream, was found to make the current distribution uniform. The concentration overpotential became larger and reached a maximum of 65 mV upstream of the fourth stage, but this was not large enough to change the current distribution. As a reference, we performed cycle analysis of a conventional SOFC/GT cycle with the amine process for recovery of CO_2 from the flue gas. The high fuel utilization SOFC/GT cycle used the SOFC pressure of 1 MPa for CO_2 liquefaction without power recovery through GT, so the net power output from GT became small, but the liquefaction power decreased. On the other hand, further output of 12.3% was produced from the high fuel utilization SOFC. Thus, we showed the possibility of about 10% higher overall power generation efficiency than that of a normal SOFC/GT equipped with the CO_2 recovery amine process. In the future it will be necessary to experimentally verify the performance of high fuel utilization SOFCs.

References

[1] A. Lokurlu, E. Riensche, F. Thom, D. Stolten, 5th European SOFC Forum, 2002, pp. 972–981.
[2] K. Onda, T. Iwanari, N. Miyauchi, K. Ito, T. Ohba, Y. Sakaki, S. Nagata, J. Electrochem. Soc. 150 (12) (2003) A1569–A1576.
[3] A. Sawata, K. Tsuneyoshi, J. Mizusaki, H. Tagawa, Solid State Ionics 40 (41) (1990) 415–420.
[4] O. Yamamoto, Y. Takeda, R. Knnno, Y. Tomita, J. Chem. Soc. Jpn. 8 (1998) 1324–1328.
[5] T. Setoguchi, K. Okamoto, K. Eguchi, H. Arai, J. Electrochem. Soc. 139 (10) (1992) 2875–2880.
[6] A. Kusu, Y. Kikuoka, T. Umagoe, K. Ueda, H. Miyamoto, N. Nakamori, Trans. Jpn. Soc. Mech. Eng. 4th Power Energy Technol. Symp. (1994) 114–118 (No. 940–56), #A17.
[7] E. Erdle, W. Donitz, R. Schamm, A. Koch, Int. J. Hydrogen Energy 17 (10) (1992) 817–819.
[8] M. Iijima, Mitsubishi Heavy Industries, personal communication.
[9] K. Marumoto, A. Aya, Y. Matsui, Trans. Jpn. Soc. Mech. Eng. 56 (532) (1990) 268–273.
[10] M. Steinberg, H.C. Cheng, F. Horn, BLN 35666 Informal Report, U.S. DOE, May 1984, pp. 5–11.